Gas vs. Condensed Phase Reactions in Nano-Thermites

Rohit J. Jacob[1], Guoqiang Jian[2], Philip M. Guerieri[1] and Michael R. Zachariah[3]*
University of Maryland, College Park, MD 20742, USA

Explosive formulations incorporating aluminum nano particles as a fuel has been extensively studied due to their low diffusion length scales and their high specific energy release compared to traditional organic formulations. In this work we evaluate the combustion product particle size distribution of nanothermites, and deduce some controlling combustion mechanisms. The results presented here show two distinct particle product distributions common to all fuel/oxidizer foumations evalauted. These two distribution contain a nanoparticle and supermicron product. From mass analysis we determine that ~90% of the product mass is comprised of the large particle population. Simple scaling arguments show that the large population cannot be formed from the vapor given the available residence time. This result implies that the majority of reaction and thus the energy release must occur in the condensed phase.

I. Introduction

NANO scale reactive composites or metastable intermolecular composites (MIC's) are an increasingly active area of research in the field of propulsion and energetics, resulting from their high energy densities, high propagation velocities and low diffusion length scales. Aumann et al. [1] were the first to show that there was a significant difference in the reactivity of nano sized thermite mixtures of Al/MoO_3 (200-500 nm) over the micron sized counterparts. When compared to the conventional mixtures, their experimentally observed reactivity was several orders of magnitude greater owing to the reduction in diffusion length scales.

Mechanistically, several theories have been postulated to explain aluminum nano particle burning including pressure build up resulting in quiescent shell rupture [2] or even spallation [3] or a more subtle diffusion mechanism [4, 5, 6] aided by the polymorphic phase transformations of the alumina shell [7] and the presence of strong electric field across it [8, 9]. One of the outstanding issues regarding the role of the oxygen carrier in the nanothermite is whether oxygen is directly released from the oxidizer or if oxygen, in the form of an anion, is transported at the interface between fuel and oxidizer. The latter case may be defined as a condensed state process, in which little or no aluminum - oxygen reaction occurs in the vapor phase. In a recent work, we stress on the importance of gas phase oxygen release on the ignition of the reactive composites [10] were we concluded that the presence of gaseous oxygen need not be a necessary prerequisite for the ignition of all nano composite thermite formulations, implying that a condensed phase reaction mechanism is still prevalent in some of the nanothermites. The current study seeks to evaluate these two competing processes i.e., condensed phase vs. vapor phase oxidation, through a post-combustion analysis of rapidly quenched product particles.

Reaction temperatures are a good parameter in measuring the extent of the reaction. Previously, methods to identify flame temperature were limited. Early approximations were based on the adiabatic flame temperatures calculated from equilibrium data assuming no energy loss [11]. For the systems of interest in the current work, there has been evidence of early reaction sintering [12], hence approximating the adiabatic flame temperature which assumes complete reaction won't give a good estimate. The literature in flame temperature measurements are rich in methods which can be classified into invasive, semi-invasive and non-invasive categories [13]. The advantage of non-invasive method is that they do not distort the temperature field of the flame thus providing better results. One such method, two color pyrometry, has been extensively studied [14-17] and has been utilized in this work for the temporal and spatial analysis of the flame.

---

[1] Graduate Research Assistant, Mechanical Engineering,

[2] Graduate Research Asst., Chemistry and Biochemistry,

[3] Professor, Chemical and Biomolecular Engineering and Chemistry and Biochemistry, 2113 Chemical and Nuclear Engineering Building.

II. Experimental Approach

Several researchers have previously investigated quenched aluminum particles to extract useful information about their burning. In this study we adapt the work of Drew et al. [18] who studied quenched aluminum particles that were cooled by helium gas. In this case we are not focusing on the transient evolution of particles as was his emphasis, but focus on events that suggest considerable condensed state processes occurring rapidlay to change the particle size distribution during burning.

In this study we ignite various nanothermites combinations on a rapidly heated fine wire, and quench product particles on a substrate at short distances away from the wire. Post-inspection by microscopy and surface analytics are subsequently performed. As an added tool to measure the flame temperatures, a hi-speed camera based multi wavelength pyrometer was recently developed to provide the temporal and spatial temperature maps of the flame, as discussed in the forthcoming sections..

A. Materials and Preparation

Commercially available Aluminum nanoparticles (ALEX) with an average particle size of 50 nm, procured from Argonide Corp., were used in this study. These particles had a core shelled structure with an active aluminum content of 70 % [5]. These ALEX nanoparticles were ultra-sonicated in a hexane suspension with three different metal oxide nanopowders. The details of the metal oxide nano powders used in this study can be found in one of our previous work [10]. After ultra-sonication, the intimately mixed thermite mixture was micro pipetted onto a platinum wire of 76 μm diameter. The three systems chosen here, exhibit varied combustion characteristics in terms of propagation speeds, pressurization rates and burn times [19, 20]. These systems were extensively studied by Sanders et al. [19] employing the pressure cell, open tray and instrumented burn tube methods to study the reaction mechanisms of these nanothermites. They concluded the importance of the presence of vapor phase/mobile components to enhance the propagation. The adiabatic temperatures vary with the choice of the thermites, with Al/WO_3 mixture exhibiting a very high adiabatic flame temperature compared to the Al/CuO formulation. From pressurization rate, and the temporal behavior of optical emission, Sullivan et al. [20] showed significant differences in case of Al/CuO and Al/WO_3 in regard to the pressure peak vs. the optical peak which shows that Al/WO_3 nano composite does not produce much gas species until the system temperatures are very high. Jian et al. [10] points out that the Al/Bi_2O_3 system ignites almost 700K below its oxygen release temperature while the Al/WO_3 system does not produce any gas within the experimental range of temperature. The Al/CuO mixture is observed to closely follow the expectation that ignition is correlated to oxygen release from the oxidizer. Apart from these variations in their respective combustion behavior, these metal oxides exhibit very different physical properties in regard to the reduced metals with copper and tungsten exhibiting higher melting and boiling temperatures compared to bismuth, as outlined in Table 1.

Table 1. Thermo-Physical properties of the nanothermite mixtures				
Thermite Mixture (Al/Metal Oxide)	Adiabatic Flame Temperatures (K)[11]	Metal Oxide decomposition point[10] (K) (±50K)	Metal Melting point (K)	Metal Boiling point (K)
Al/CuO	2843	975	1357	2843
Al/WO_3	3253	-	3695	5933
Al/Bi_2O_3	3319	1620	545	1837

These dissimilarities provide the motivation for choosing these three materials for the current work. All three, show significantly different behavior in terms of ignition point, combustion intensity, physical properties and gas release. The question is how the nature of the product distribution would vary for these disparate systems, and if the analysis of the product could shed some light on their respective mechanisms.

B. T-Jump Wire Ignition and Particle Collection

American Institute of Aeronautics and Astronautics

The experiment was conducted in air. 76 μm diameter platinum wire (Omega Engineering Inc.) coated with the nanothermite was resistively heated using a high voltage electric pulser. For each run a pulse width of 3 ms was used giving a heating rate of 2×10^5 K/s. The details of the wire heating system comprising the mass spectrometer and power source can be obtained in another work by Zhou et al. [21]. In these set of experiments the primary modification was the ability to capture reproducibly, post-combustion material on substrates. The collecting substrate was a separately attached Scanning Electron Microscopy (SEM) stage such that by moving the Z direction micrometer we could collect the product particles on the substrate at distances on the order of millimeters away from the. A similar arrangement was used for the Transmission Electron Microscopy (TEM) samples. A high speed digital camera (Phantom V12.1) was used to capture the video of the reaction from which characteristic transit times could be extracted.

C. High-speed, two color Pyrometry

Two-color pyrometry has been well documented in several previous publications [13-17] and is not repeated here. The basic experiment is schematically shown in the Figure 1. The operating procedure involves computing the ratio of the light intensities at two different wavelengths and computing the temperature using Planck's law. Since this is a ratio calculation, and as the wavelengths are reasonably close, we can approximate the wavelength specific emissivity of the particles in the flame to be equal (i.e gray body approximation). The light emitted by the flame is collimated using a biconvex lens and split with a 50-50 plate beamsplitter. The transmitted beams passed through 700 nm and 800 nm band pass filters, and the two wavelength selected images were focused on a high speed video camera (Phantom V12.1). The system was calibrated using a Black Body source from Newport Corp. (Model 67030).
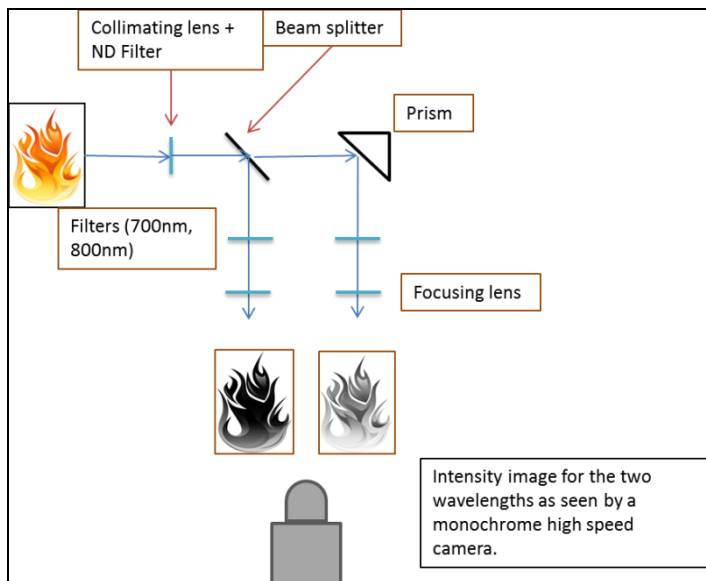
Figure 1. Pictorial representation of the High-speed Pyrometry setup.

III.   Results and Discussion

A. Electron Microscopy of Post-combustion Products

A Hitachi SU 70 SEM and a JEOL FEG TEM was used for the electron microscopy evaluation. Particles were collected at two distinct separation distances to make a fair comparison of the particle evolution. The SEM images obtained are shown in the subsequent images with an approximate transit time to the substrate, obtained by performing high speed video imaging on the emission from individual particle trajectories.

B. Nanothermite systems: Al/CuO, Al/WO$_3$ and Al/Bi$_2$O$_3$

American Institute of Aeronautics and Astronautics

Figure 2 show moderate and high magnification SEM images of the residue collected for the Al/CuO case. The residue was collected at two different substrate separations (1 mm and 3 mm) from the wire and the representative image shown in Figure 2 is for the near case. From these images we can see that a significant number of large particles (*in comparison to the nanoscale starting materials*) have formed from the thermite reaction, some of which are as large as 20 μm. Also, this phenomenon is observed at both separation distances with a particle size on the order of 10 microns. At still higher magnifications, using a JEOL FEG TEM we observe a layer of much finer particles as shown in Figure 2b.
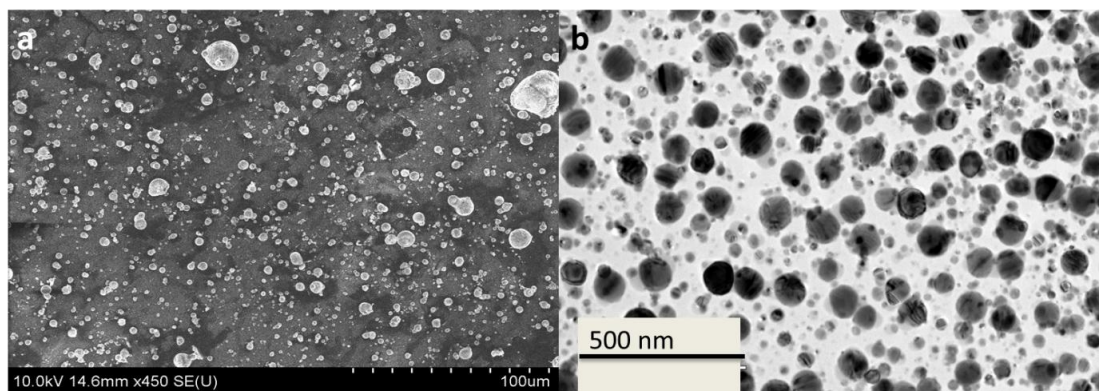
Figure 2. *Post-combustion SEM/TEM images of Al/CuO nanothermite collected at 1 mm.*
a.) Low magnification b.) High **Magnification TEM**

This set of experiments were then broadened to include the Al/Bi$_2$O$_3$ and Al/WO$_3$. The key feature, the presence of two disparate particle populations, could be observed for these cases as well, but are not shown.

C. Post-combustion Products: Large vs. Small Particle Products and its Significance on Mechanism

The microscopy images showed there were two particle populations. Our first consideration is to understand the relative importance of these two populations in the context of a mechanism, by estimating the relative mass distributions. To do this we employed digital image processing using the software ImageJ [22]. The SEM image is post processed by adjusting the image threshold to single out the large particles against the background, which enabled us to determine the average size of the particles. For this calculation, the background was assumed to be composed of a single layer of 50 nm nano particles (based on the TEM images). This enables us, assuming spherical geometry and total aerial coverage, to estimate the volume fraction of each population.

The image processing results gives an average particle size of 2.5 μm. Even though the aerial coverage of the large particles are much smaller than the nanosized particles, their larger size comprise ~85% of the volume. Assuming density is roughly constant between the two particle populations, the volume ratio is also approximately the mass ratio. Similar analysis for Al/WO$_3$ and Al/Bi$_2$O$_3$ gave results that were experimentally essentially indistinguishable i.e. 90 and 85 % respectively. These results are summarized in Table 2 and are qualitatively consistent with a very recent study by Poda et al. [23], wherein they recover product samples from the interior of a closed bomb cell. They also observed large particles in the products that deviate substantially from the nanosized precursors.

American Institute of Aeronautics and Astronautics

Table 2. Image processed determination of the ratio of micron and nanoparticle products after combustion
.

Thermite System	**Micron to nano volume ratio in the products**	**Volume percentage (micron)**
Al/CuO	5.7	85 %
Al/WO$_3$	9	90 %
Al/Bi$_2$O$_3$	6.2	85 %
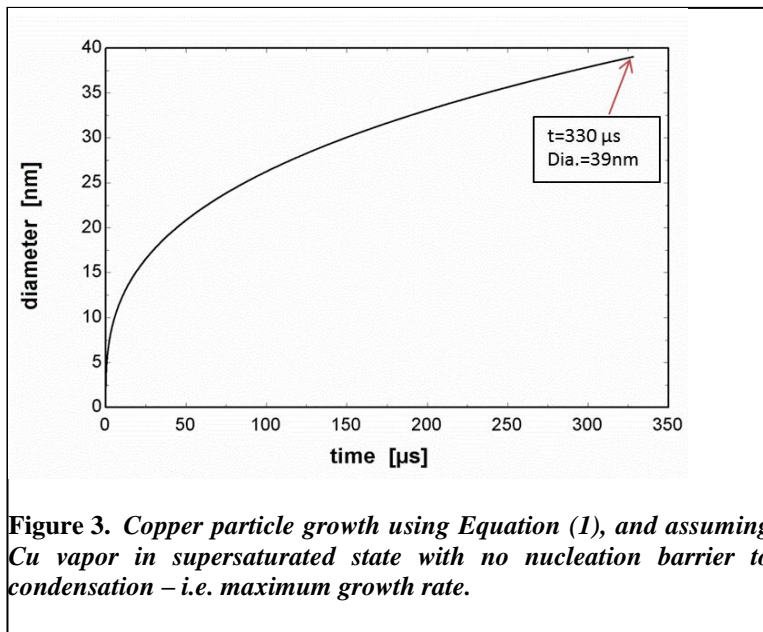
Figure 3. *Copper particle growth using Equation (1), and assuming Cu vapor in supersaturated state with no nucleation barrier to condensation – i.e. maximum growth rate.*

Thus we may conclude that the bulk of the chemistry and energy release must pass through a mechanism that leads to the larger particles as opposed to the smaller nanoparticle products.

Most of these small particles are highly spherical, implying that they were in the liquid state at some point in their history, and were rapidly quenched on the substrate. From Table 1 for the Al/CuO mixture, we can deduce that copper metal, a product of the redox reaction, would vaporize since the adiabatic flame temperature is near the boiling point of the metal. This allows us to post the question: How large a particle can be grown from the vapor in the transit time from the wire to substrate? To estimate the largest possible growth rate we assume that the copper vapor is in a supersaturated state with no nucleation barrier. Here we conservatively assume to maximize growth rate that the entire copper product is in the vapor, which is actually a factor of two higher than what equilibrium would predict. The presence of copper vapor is further supported by ref [6] which finds copper peaks during the combustion of the Al/CuO nanothermite mixture in a mass spectrometer. Without a nucleation barrier, nucleation and growth follows the aerosol coagulation equation in the free molecule regime [24]. The total mass of copper is estimated from the amount coated on the wire, which is approximately 0.1mg, and the stoichiometry of the mixture. The expansion volume for the products of the thermite reaction was considered as half the volume of the cylinder that forms between the wire and the collecting substrate i.e., the axis of the cylinder lies along the wire. This was evaluated for the near substrate condition, as that gives the maximum initial monomer concentration, thereby giving the fastest rate of coagulation compared to the far substrate case.

For simplicity of calculation we assume a constant collision constant, K= 5E-10 cc/s [24] so that the Smulochowski population balance is reduced to the following equation 1 [24]:

$$N_\infty(t) = \frac{N_\infty(0)}{1 + K * N_\infty(0) * t / 2} \qquad (1)$$

5

American Institute of Aeronautics and Astronautics

Where, $N_\infty(0)$ is the initial monomer concentration (#/cc), $N_\infty(t)$ is the total particle concentration at time t (#/cc), t is time (s). The solution for the average particle diameter as function of time can be obtained by employing a simple volume conservation using the Van der Waals radius of copper (~0.14 nm) and assuming an initial monomer concentration equal to the maximum vapor phase concentration of Cu.

Figure 3 shows the growth of particles as a function of time at effectively the maximum collision rate. We see that at ~330 µs, which corresponds to what we believe is the transit time for the particles to the substrate (based on the hi-speed video approximated transit times), the nominal particles size should be about ~40 nm. This is reasonably consistent given the approximations in our calculation with the TEM results for the small particles. *But more significantly it says that there is no way that the large micron size particles, which will be recalled constitute the bulk of the mass, can form from the vapor.* In their work on arrested reactive milling, Schoenitz et al. [25] also found large particles in the product of micron size Al/MoO_3 combustion. In a previous work by Sullivan et al. [26], real time X-ray phase contrast imaging was performed to substantiate the formation of sintered particles early in the reaction. They found large particles forming rapidly and early in the reaction. Thus we believe the large particles correspond to aluminum-metal oxide reaction that must have occurred in the condensed phase. Such particles have also been formed during flash ignition of nano aluminum thermites [27], thus strengthening a common reaction feature irrespective of the environment, ignition mechanism or heating rate.

D. Pyrometry Results

Multi wavelength pyrometer was developed to visualize the spatial and temporal temperature fields. This was done for the case of Al/CuO and the results are presented Figure 4. From visual inspection of the images, we can see that there are few regions that show exceptionally high temperatures. These are artifacts and may represent the chemical species emission, which disrupt the gray body emission ratio. Nevertheless, an approximate temperature of the flame based on the temperature map gives values in the range of ~2500 K. We emphasize that this temperature value is not the average of the individual points but just from a visual analysis. The measured value corresponds reasonably well to the temperature reported in [13] of 2150 ± 100 K but offers higher resolution. In both cases the measured temperatures are below the adiabatic flame temperature.

E. Phenomenological Mechanism

We believe a generic mechanism can be attributed to these results. The vast majority of the particle products studied are at least two orders of magnitude larger in diameter and cannot be formed from a vapor condensation mechanism. Thus the bulk of the energetic heat release must come from a condensed state reaction. The large particles are the result of sintering, hence we can argue that their temperature would, at some point in their evolution, be above the melting point of the alloy formed due to complete/incomplete oxidation or diffusion of species [28]. As the nano
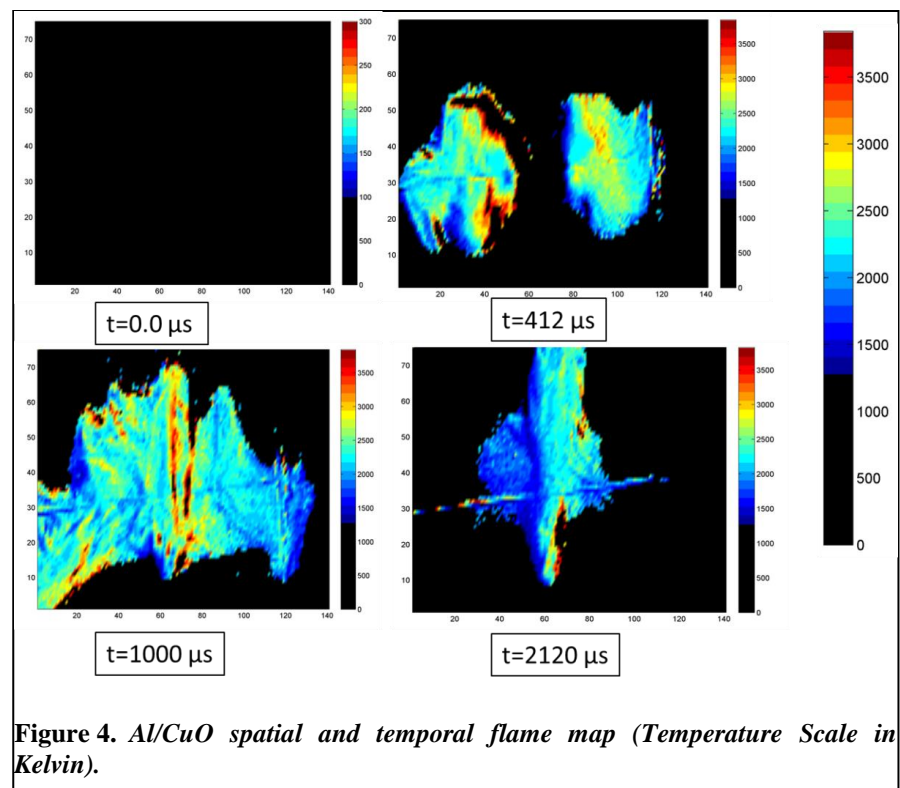
Figure 4. *Al/CuO spatial and temporal flame map (Temperature Scale in Kelvin).*

6

American Institute of Aeronautics and Astronautics

particles grow from the vapor phase, they would be expected to be scavenged by the larger particles by coagulation/coalescence.

From our coagulation calculation it is evident that the large particles cannot be formed from the vapor phase. In one of our previous publications, we discussed the possibility of early sintering of the reactants due to the heat released by the exothermic reaction, termed Reactive Sintering [12]. As outlined in references [12] and [26], the reaction initiates at the reactant contact points. Once the exothermic oxidation reaction initiates, the system temperature and results in significant volatilization which will subsequently nucleate and grow depending on the transit time. The product, which is molten, is thus driven by coalescence and surface tension to be highly spherical. Based on the temperature measurements, we belive the reaction temperature is below the adiabatic flame temperature and although the radiation heat losses may play an important part, such a reduction in temperature may also be attributed to an incomplete reaction, possibly due to sintering effects which corsen the particles and increase diffusion distances.

In another recent work [29], these core shelled Aluminum nano particles were studied in a Dynamic TEM at the Livermore National Labs were a pulsed laser was used to heat up these nano particle aggregates at rates of 10^{11} K/s, far higher than our wire experiments. They observed that the aggregates sintered on a time scale of 10 ns which is three orders of magnitude lower than the reaction time scales that were reported in [30] where a shock tube was employed. Similar results were also found through MD simulations [28] and thus we can safely say that there is a propensity for the nano particles to aggregate into larger sizes before the reaction can initiate and we believe that the large particles seen in this study and elsewhere in other studies are formed as a result of such pre combustion sintering. The small particles that we see in this study can correlate to a vapor phase mechanism, where the aluminum oxidizes in the vapor and coagulate following the growth law simultaneously with the reduced metal.

IV. Conclusion

In this work, where the product particles from thermite reactions were analyzed to obtain mechanistic information. The analysis shows the presence of two disparate particle size distributions. The large particles which comprise the bulk of the product on a mass basis, cannot by scaling argumnts, be formed from a vapor phase condensation mechanism, given the available residence time. Thus we conclude that the primary reaction mechanism in nanothermites is through a condensed state route. A high speed two color pyrometer was developed to spatially and temporally resolve the flame temperature, which indicated reaction temperatures below the adiabatic temperature. These results also suggests a possible reason why nanostructured particle may not react as fast as might be expect, due to the rapid sintering during the reaction process.

Acknowledgments

References

[1]C. E. Aumann; G. L. Skofronick; J. A. Martin, Journal of Vacuum Science & Technology B 13 (3) (1995) 1178-1183 10.1116/1.588232.

[2]A. Rai; D. Lee; K. H. Park; M. R. Zachariah, Journal of Physical Chemistry B 108 (39) (2004) 14793-14795 10.1021/jp0373402.

[3]V. I. Levitas; B. W. Asay; S. F. Son; M. Pantoya, Applied Physics Letters 89 (7) (2006) 10.1063/1.2335362.

[4]A. Rai; K. Park; L. Zhou; M. R. Zachariah, Combustion Theory and Modelling 10 (5) (2006) 843-859 10.1080/13647830600800686.

[5]S. Chowdhury; K. Sullivan; N. Piekiel; L. Zhou; M. R. Zachariah, Journal of Physical Chemistry C 114 (20) (2010) 9191-9195 10.1021/jp906613p.

[6]G. Jian; N. W. Piekiel; M. R. Zachariah, Journal of Physical Chemistry C 116 (51) (2012) 26881-26887 10.1021/jp306717m.

[7]M. A. Trunov; M. Schoenitz; E. L. Dreizin, Combustion Theory and Modelling 10 (4) (2006) 603-623 10.1080/13647830600578506.

[8]B. J. Henz; T. Hawa; M. R. Zachariah, Journal of Applied Physics 107 (2) (2010) 10.1063/1.3247579.

[9]K. S. Martirosyan; I. A. Filimonov; D. Luss, Aiche Journal 50 (1) (2004) 241-248 10.1002/aic.10022.

[10]G. Q. Jian; S. Chowdhury; K. Sullivan; M. R. Zachariah, Combustion and Flame 160 (2) (2013) 432-437 10.1016/j.combustflame.2012.09.009.

[11]J. A. Puszynski, Journal of Thermal Analysis and Calorimetry 96 (3) (2009) 677-685 10.1007/s10973-009-0037-0.

[12]K. T. Sullivan; N. W. Piekiel; C. Wu; S. Chowdhury; S. T. Kelly; T. C. Hufnagel; K. Fezzaa; M. R. Zachariah, Combustion and Flame 159 (1) (2012) 2-15 10.1016/j.combustflame.2011.07.015.

[13]K. Kappagantula; C. Crane; M. Pantoya, Review of Scientific Instruments 84 (10) (2013) 10.1063/1.4822118.

[14]J. M. Densmore; M. M. Biss; K. L. McNesby; B. E. Homan, Applied Optics 50 (17) (2011) 2659-2665

[15]J. M. Densmore; B. E. Homan; M. M. Biss; K. L. McNesby, Applied Optics 50 (33) (2011) 6267-6271

[16]M. R. Weismiller; J. G. Lee; R. A. Yetter, Proceedings of the Combustion Institute 33 (2011) 1933-1940 10.1016/j.proci.2010.06.094.

[17]J. M. Densmore; M. M. Biss; B. E. Homan; K. L. McNesby, Journal of Applied Physics 112 (8) (2012) 5 10.1063/1.4762009.

[18]C.M. Drew; A.S. Gordon; R.H. Knipe, Heterogenous Combustion, Progress in Astronautics and Aeronautics 15 (1964) 17-39 10.2514/5.9781600864896.0017.0039

[19]V. E. Sanders; B. W. Asay; T. J. Foley; B. C. Tappan; A. N. Pacheco; S. F. Son, Journal of Propulsion and Power 23 (4) (2007) 707-714 10.2514/1.26089.

[20]K. Sullivan; M. R. Zachariah, Journal of Propulsion and Power 26 (3) (2010) 467-472 10.2514/1.45834.

[21]L. Zhou; N. Piekiel; S. Chowdhury; M. R. Zachariah, Rapid Communications in Mass Spectrometry 23 (1) (2009) 194-202 10.1002/rcm.3815.

[22]ImageJ   http://rsb.info.nih.gov/ij/

[23]A.R. Poda; R.D. Moser; M.F. Cuddy; Z. Doorenboos; B.J. Lafferty; C.A. Weiss Jr.; A. Harmon; M.A. Chappell; J.A. Steevens, Journal of Nanomaterials and Molecular nanotechnology 2 (1) (2013) 10.4172/2324-8777.1000105

[24]S. K. Friedlander, Smoke Dust and Haze, Fundamentals of Aerosol Dynamics, Oxford University Press, (2000)

[25]. M. Schoenitz; T. S. Ward; E. L. Dreizin, Proceedings of the Combustion Institute 30 (2005) 2071-2078 10.1016/j.proci.2004.08.134.

[26]K. T. Sullivan; W. A. Chiou; R. Fiore; M. R. Zachariah, Applied Physics Letters 97 (13) (2010) 10.1063/1.3490752.

[27]Y. Ohkura; P. M. Rao; X. L. Zheng, Combustion and Flame 158 (12) (2011) 2544-2548 10.1016/j.combustflame.2011.05.012.

[28].P. Chakraborthy, M.R Zachariah, Combustion and Flame (2013), Article in Press 10.1016/j.combustflame.2013.10.017

[29]G. C. Egan, K. T. Sullivan, T. LaGrange, B. W. Reed, and M. R. Zachariah, Manuscript in preparation

[30]T. Bazyn; H. Krier; N. Glumac, Combustion and Flame 145 (4) (2006) 703-713 10.1016/j.combustflame.2005.12.017.